Electronic Supplementary Material (ESI) for CrystEngComm.

Supporting Information:

Imine-tautomers of Aminothiazole Derivatives: Intriguing aspects of Chemical Reactivities

Nithi Phukan, Jubaraj B. Baruah*

Department of Chemistry, Indian Institute of Technology Guwahati,

Guwahati-781 039, Assam, India, juba@iitg.ernet.in

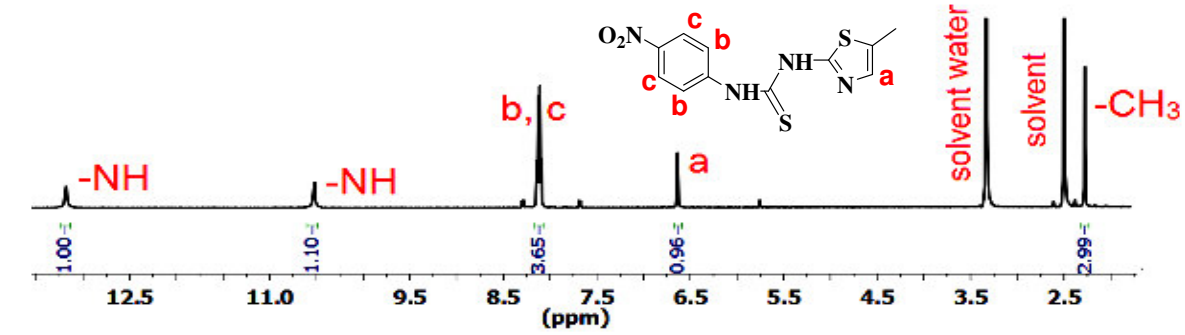

(a)

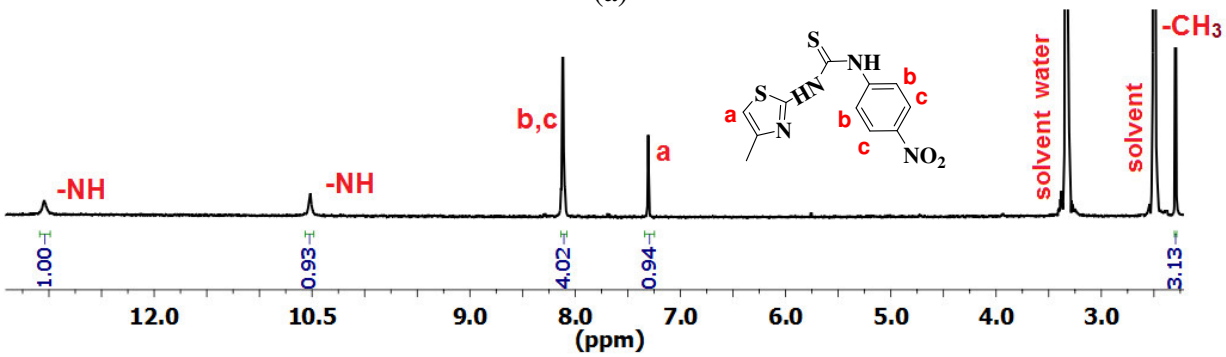

(b)

Figure S1: ^{1}H-NMR (600 MHz, DMSO-d^{6}) spectra of (a) **L^{1}** and (b) **L^{2}**

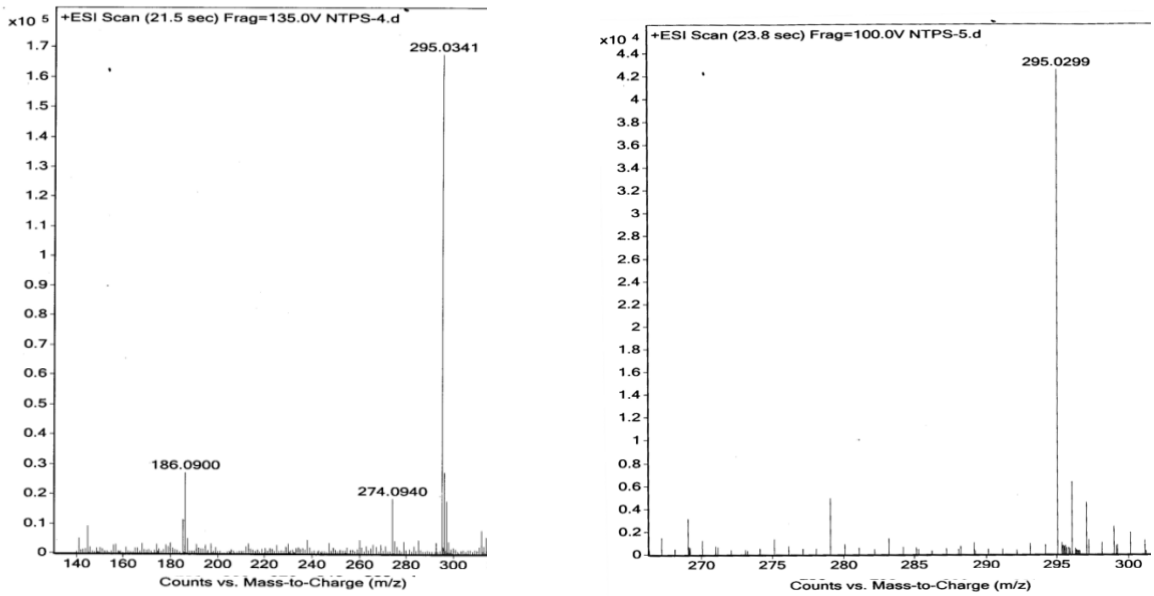

(a) (b)

Figure S2: ESI mass spectra of (a) $\mathbf{L^1}$ and (b) $\mathbf{L^2}$

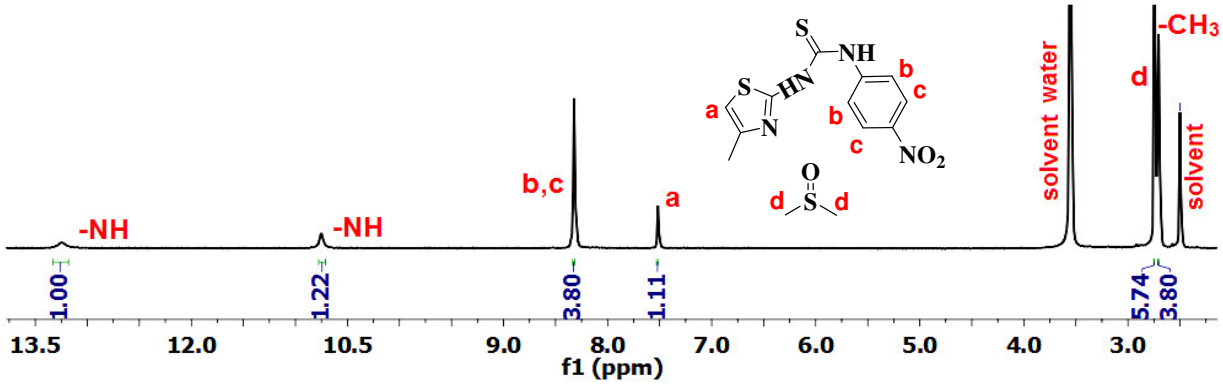

Figure S3: ^{1}H-NMR spectrum (400 MHz, DMSO-d^6) of DMSO solvate **1a**.

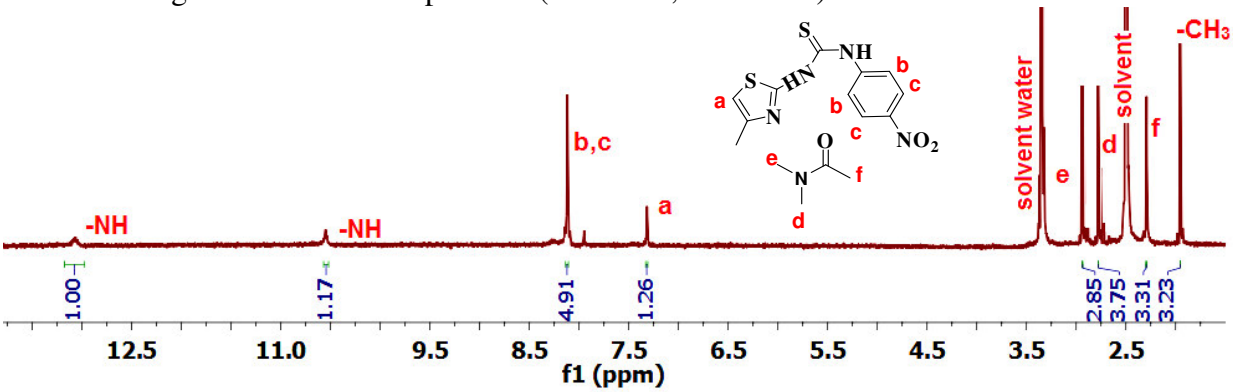

Figure S4: ^{1}H-NMR spectra (400 MHz, DMSO-d^6) of **2a**.

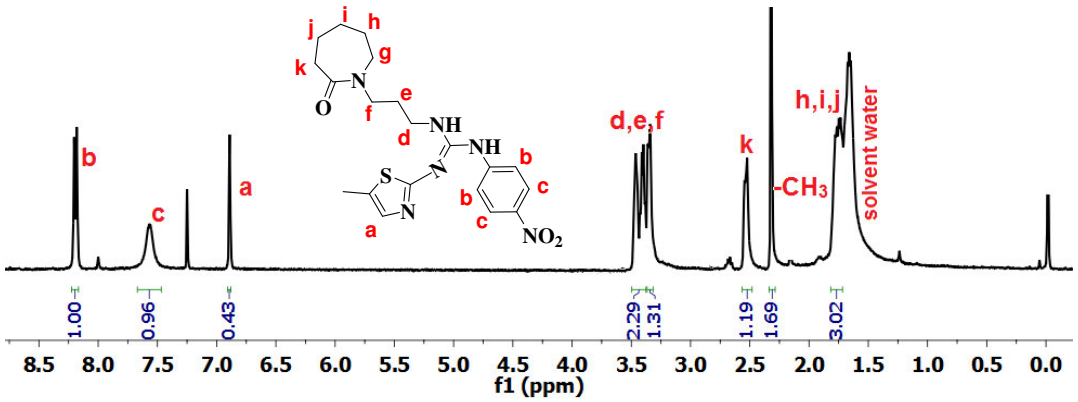

Figure S5: ^{1}H-NMR spectra (400 MHz, $CDCl_3$) of **3a**.

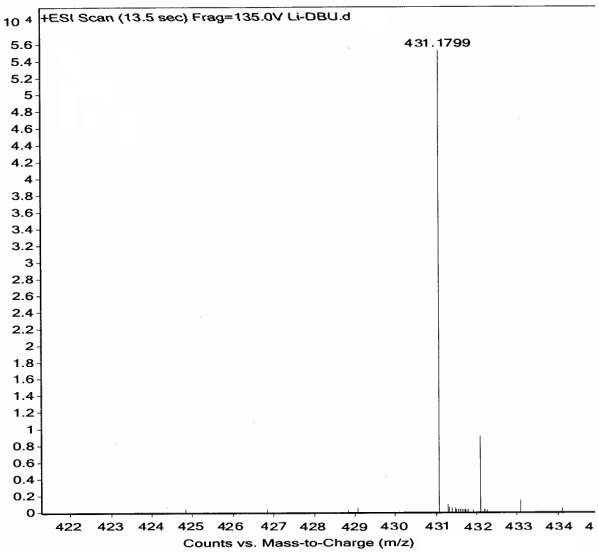

Figure S6: ESI mass spectra of **3a**.

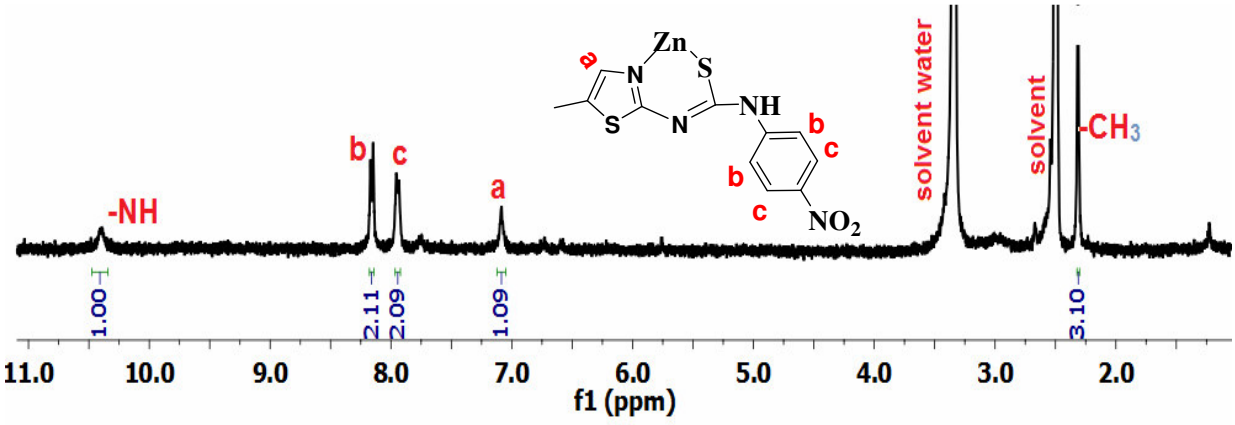

(a)

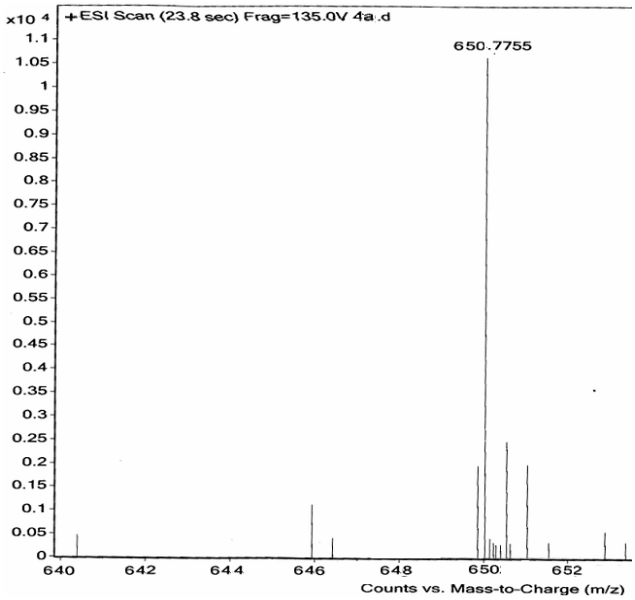

(b)

Figure S7: (a) ^{1}H-NMR spectra (400 MHz, DMSO-d^{6}) of complex **4**. (b) ESI mass spectrum of **4**.

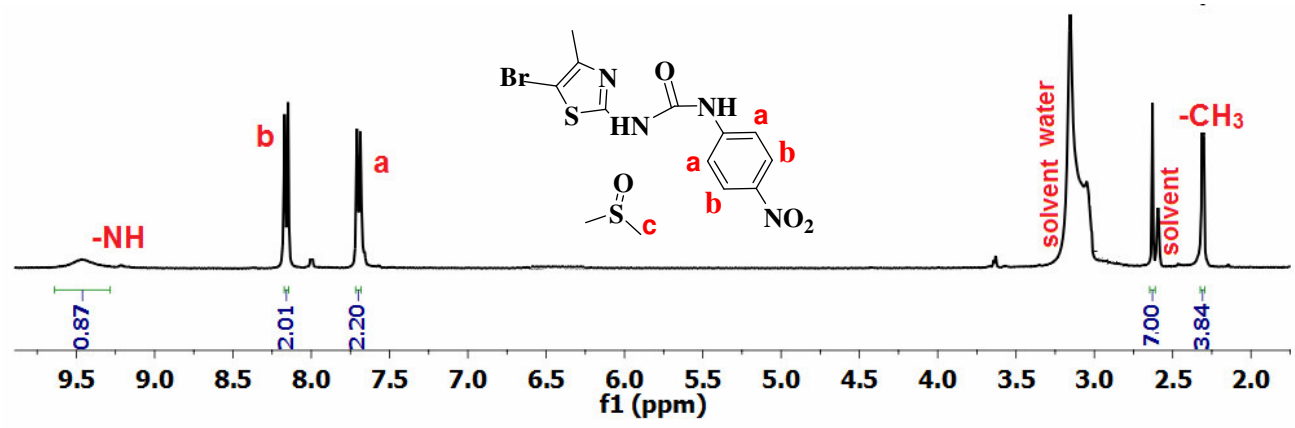

Figure S8: ^{1}H-NMR spectra (400MHz, DMSO-d^{6}) of **1b**.

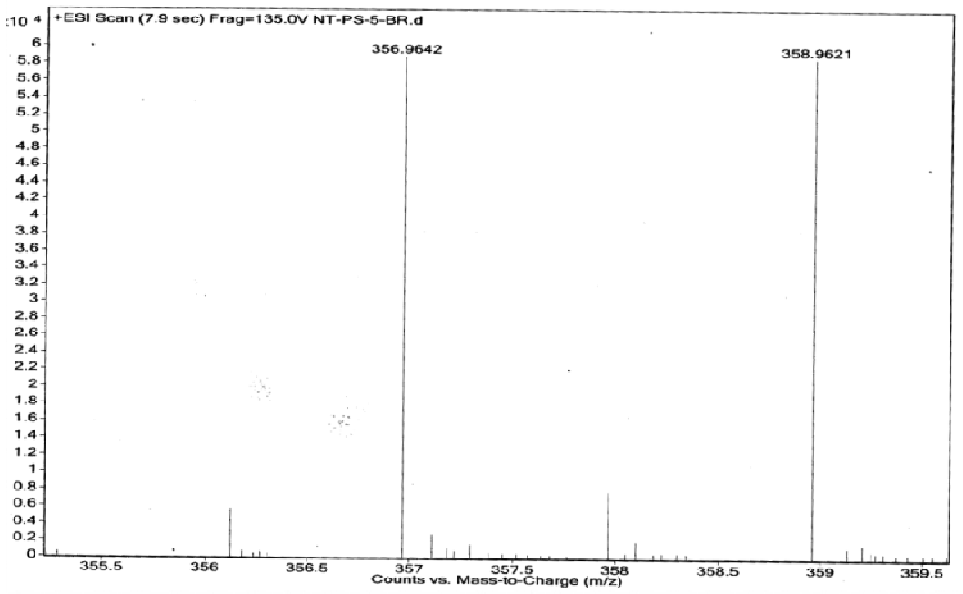

Figure S9: ESI mass spectra of **1b.**

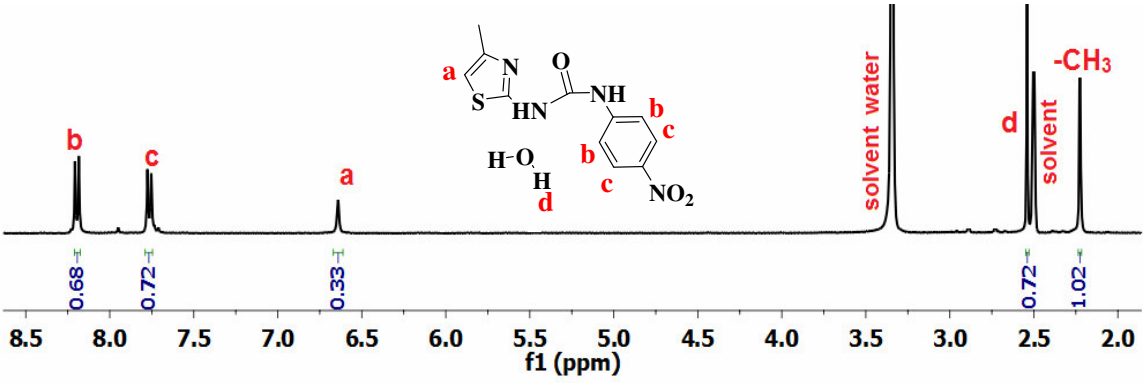

Figure S10: ^{1}H-NMR spectra (400MHz, DMSO-d^{6}) of **2b**.

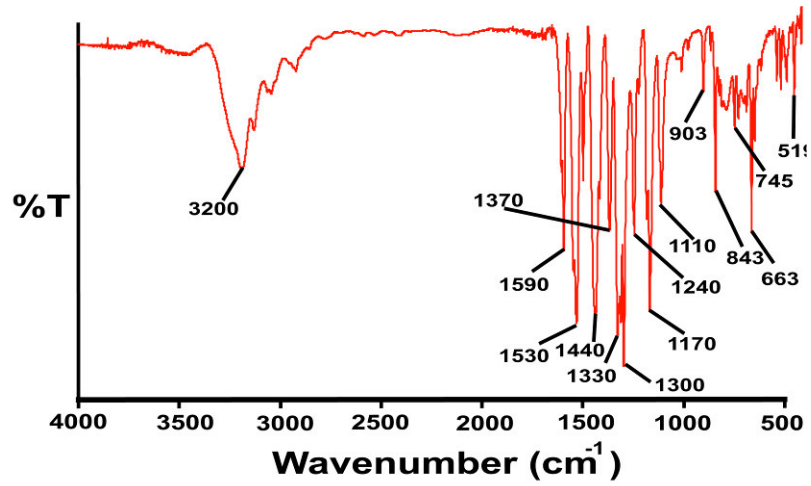
%T
3200
1370
1590
1530
1440
1330
1300
1240
1170
1110
903
843
745
663
4000
3500
3000
2500
2000
1500
1000
500
Wavenumber (cm-1)

(a)

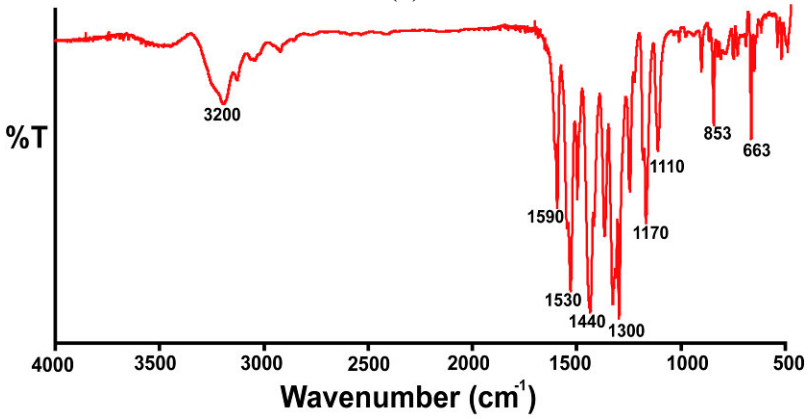
%T
3200
1590
1530
1440
1300
1170
1110
853
663
4000
3500
3000
2500
2000
1500
1000
500
Wavenumber (cm-1)

(b)

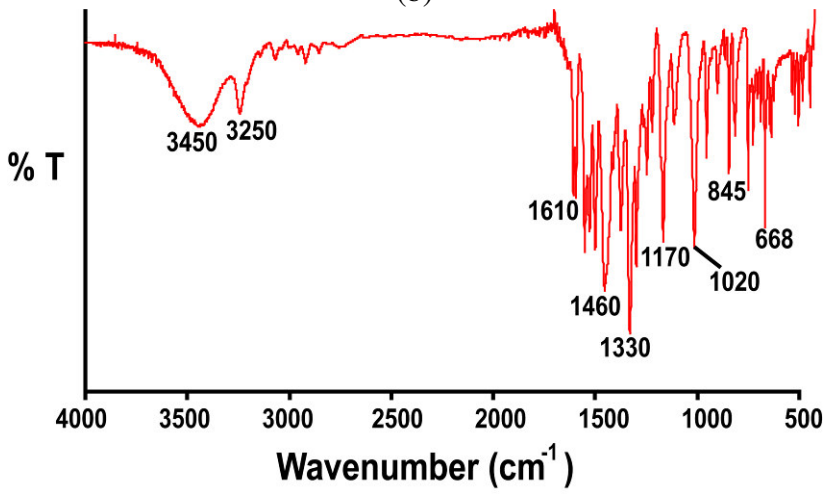
% T
3450
3250
1610
1460
1330
1170
1020
845
668
4000
3500
3000
2500
2000
1500
1000
500
Wavenumber (cm-1)

(c)

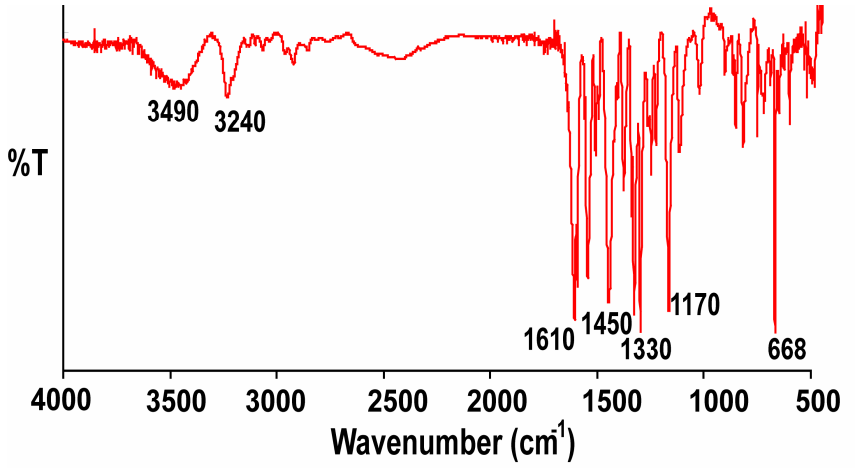
%T
3490
3240
1610
1450
1330
1170
668
4000
3500
3000
2500
2000
1500
1000
500
Wavenumber (cm-1)

(d)

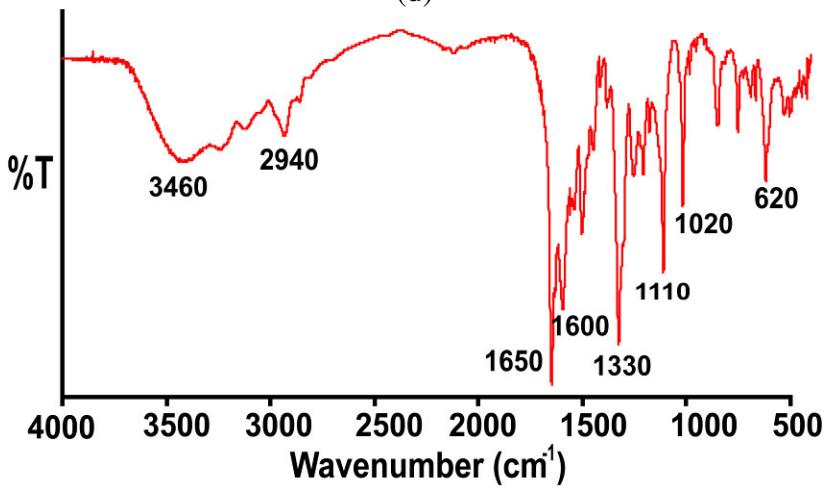
%T
3460
2940
1650
1600
1330
1110
1020
620
4000
3500
3000
2500
2000
1500
1000
500
Wavenumber (cm-1)

(e)

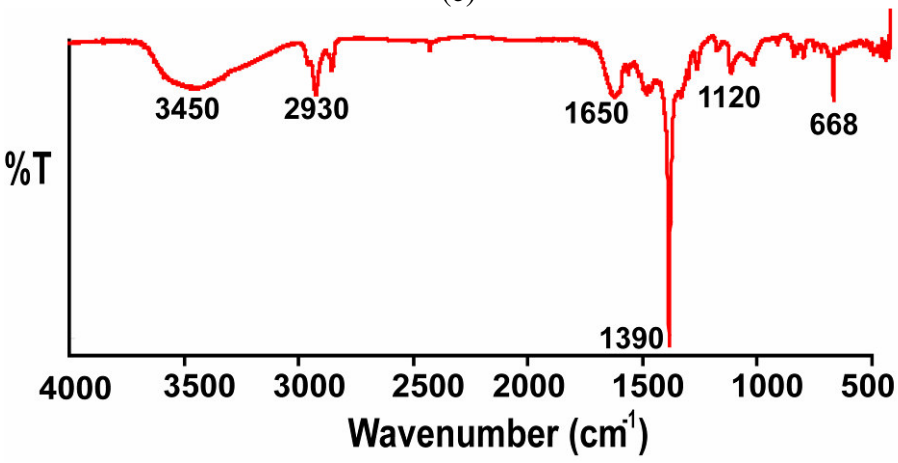
%T
3450
2930
1650
1390
1120
668
4000
3500
3000
2500
2000
1500
1000
500
Wavenumber (cm-1)

(f)

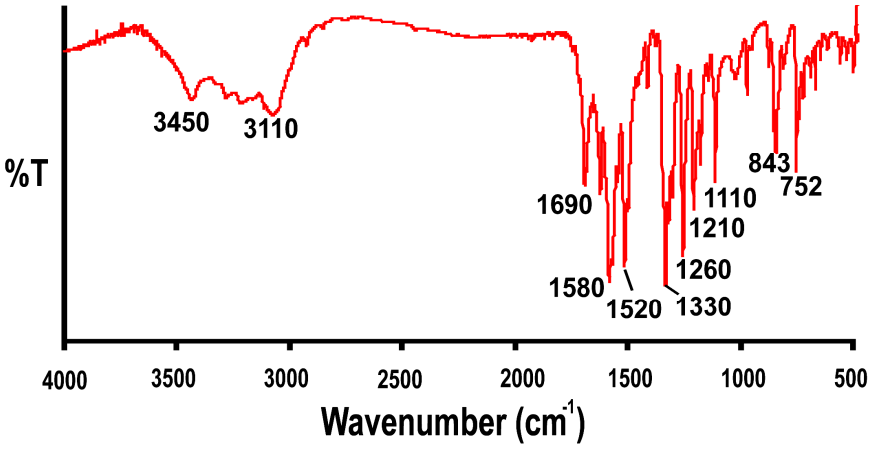

(g)

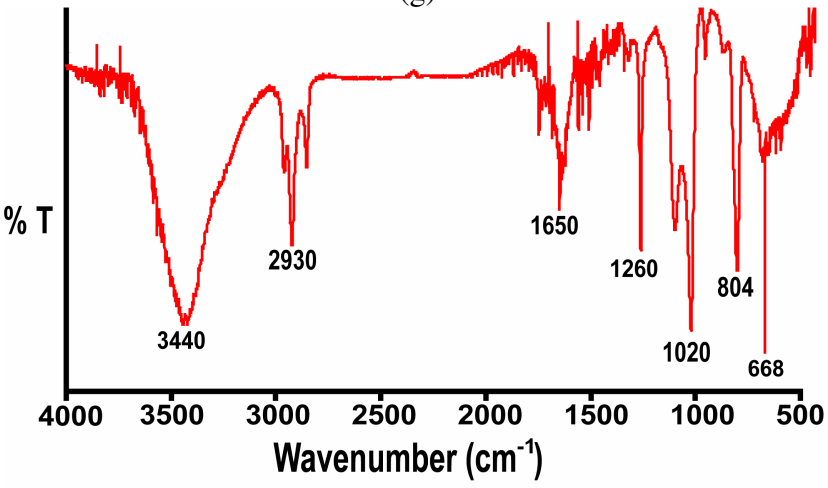

(h)

Figure S11: FT-IR spectra (KBr, cm^{-1}) of (a) $\mathbf{L^1}$; (b) $\mathbf{L^2}$ **(c) 1a;** (d) **2a;** (e) **3a;** (f) **4; (g) 1b; (h) 2b.**

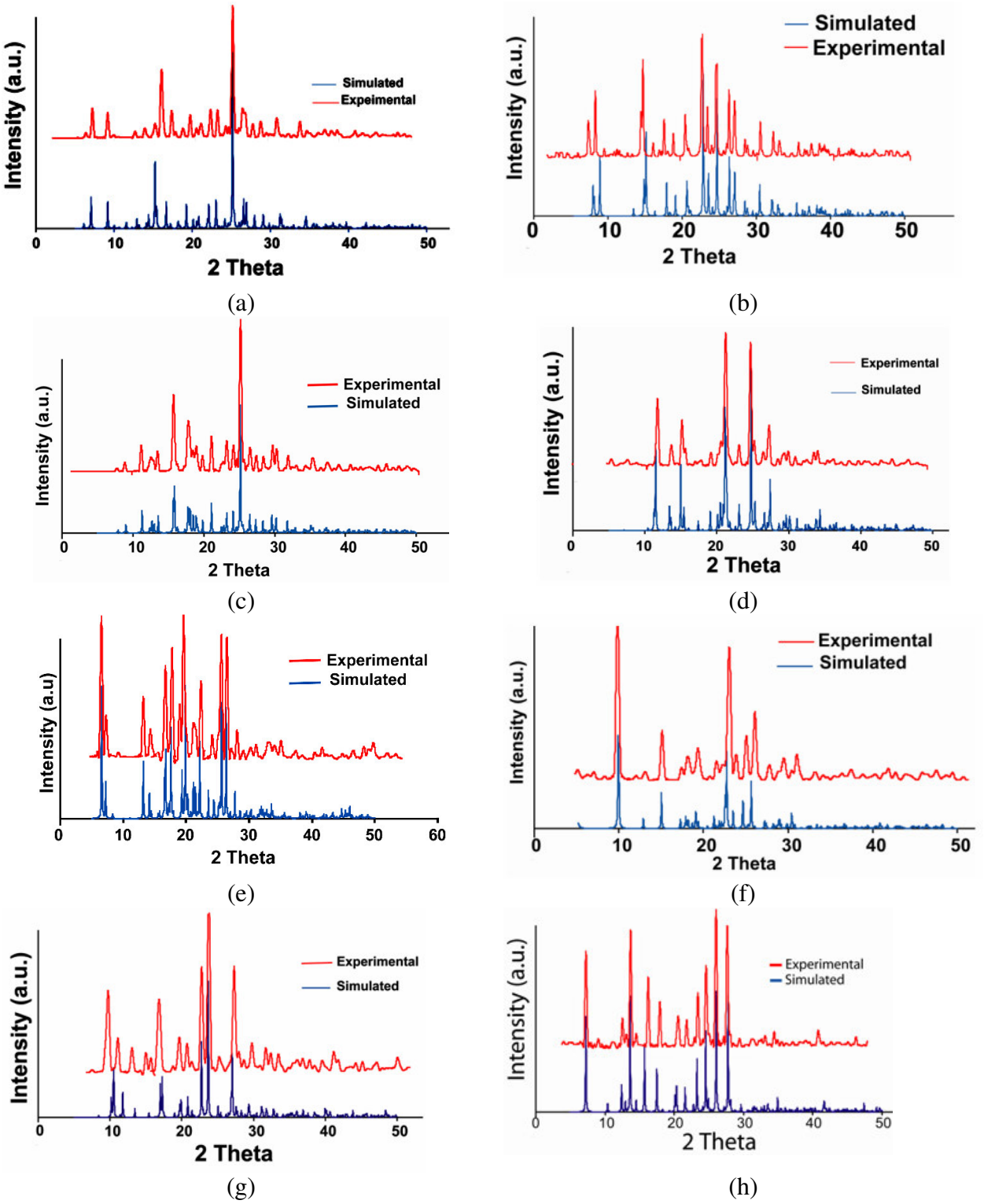

Figure S12: Powder XRD patterns of (a) $\mathbf{L^1}$ (b) $\mathbf{L^2}$ (c) **1a;** (d) **2a;** (e) **3a;** (f) **4** (g) **1b** (h) **2b**.(top one are experimental pattern and lower one are generated from crystallographic information files)

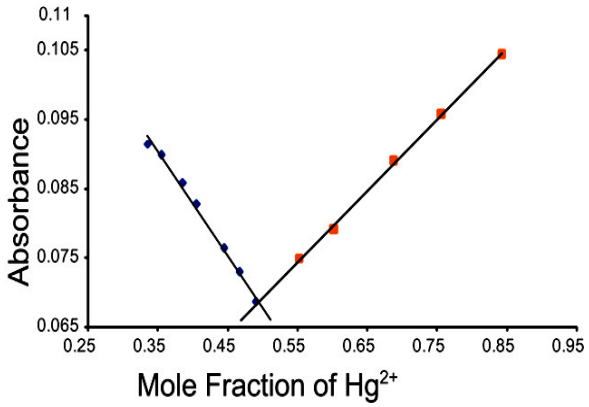

Figure S 13: Job plot for the determination of the stoichiometry of $\mathbf{L^1}$ and Hg^{2+} in the complex (absorbance at 355nm).

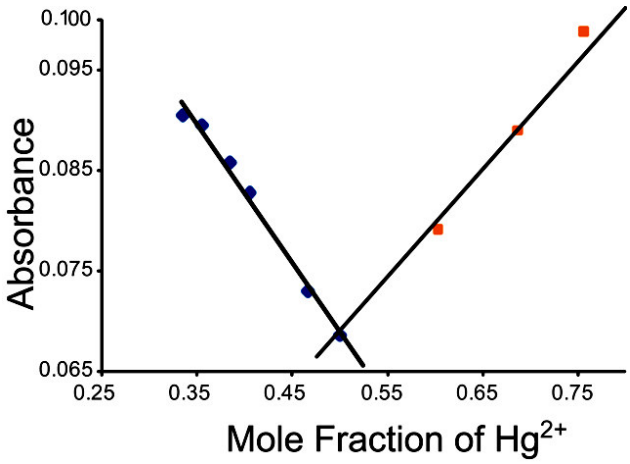

Figure S14: Job plot for the determination of the stoichiometry of $\mathbf{L^2}$ and Hg^{2+} in the complex (absorbance at 350 nm).

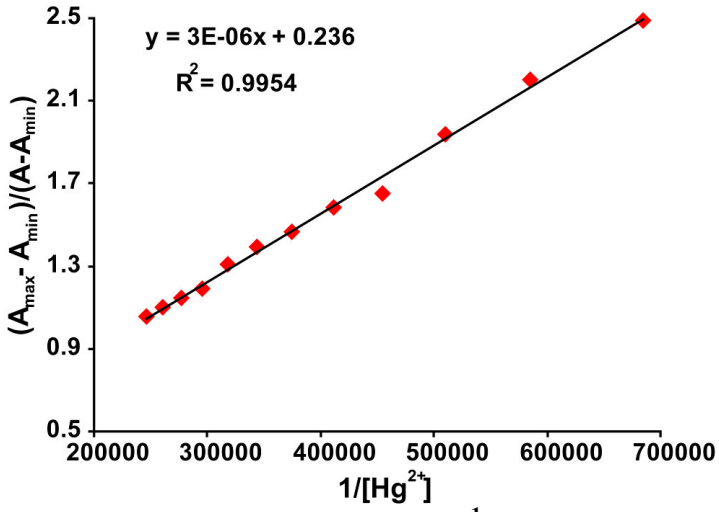

Figure S15: Benesi–Hildebrand plot of $\mathbf{L^1}$ for titration with Hg^{2+}.

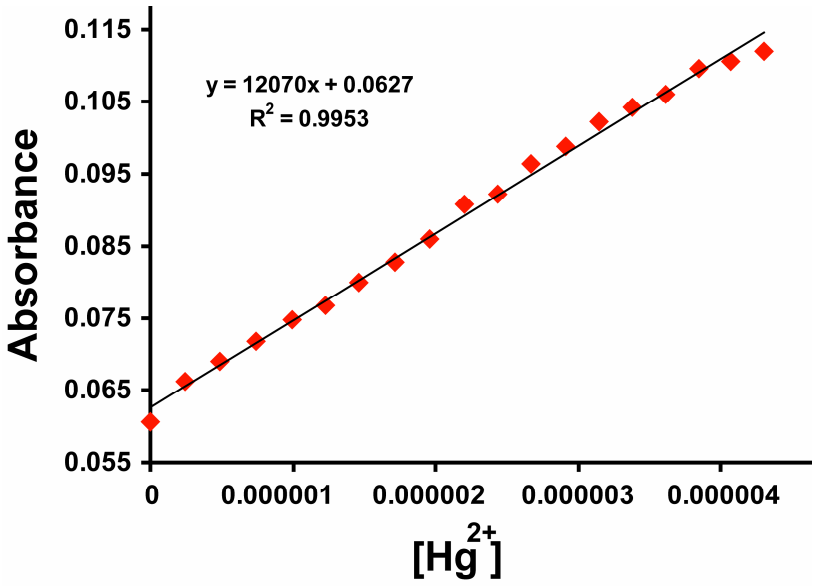

Figure S16: Absorbance versus concentration plot for measuring the detection limit (3σ/k, σ= 0.0000753) of Hg^{2+} by $\mathbf{L^1}$.

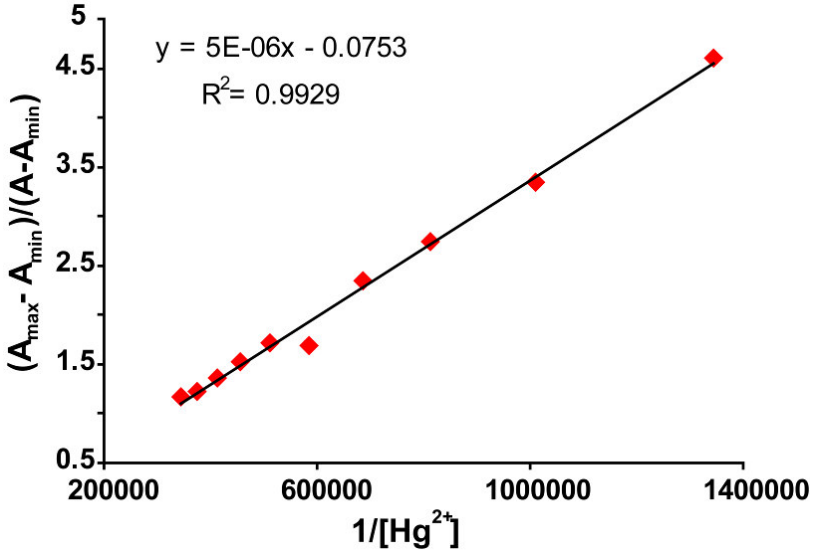

Figure S17: Benesi–Hildebrand plot of $\mathbf{L^2}$ for titration with Hg^{2+}.

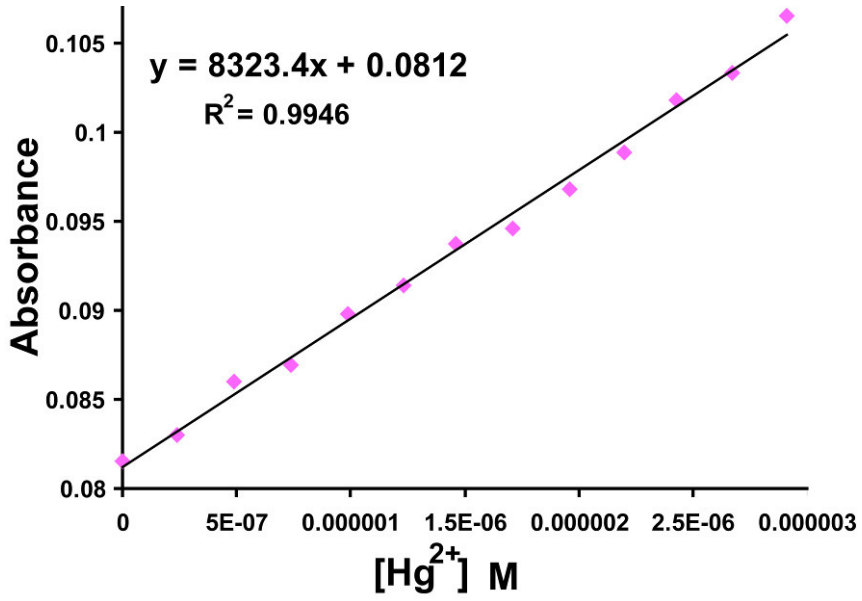

Figure S18: Absorbance versus concentration plot for measuring the detection limit (3σ/k, σ= 0.000101222) of Hg^{2+} by $\mathbf{L^2}$

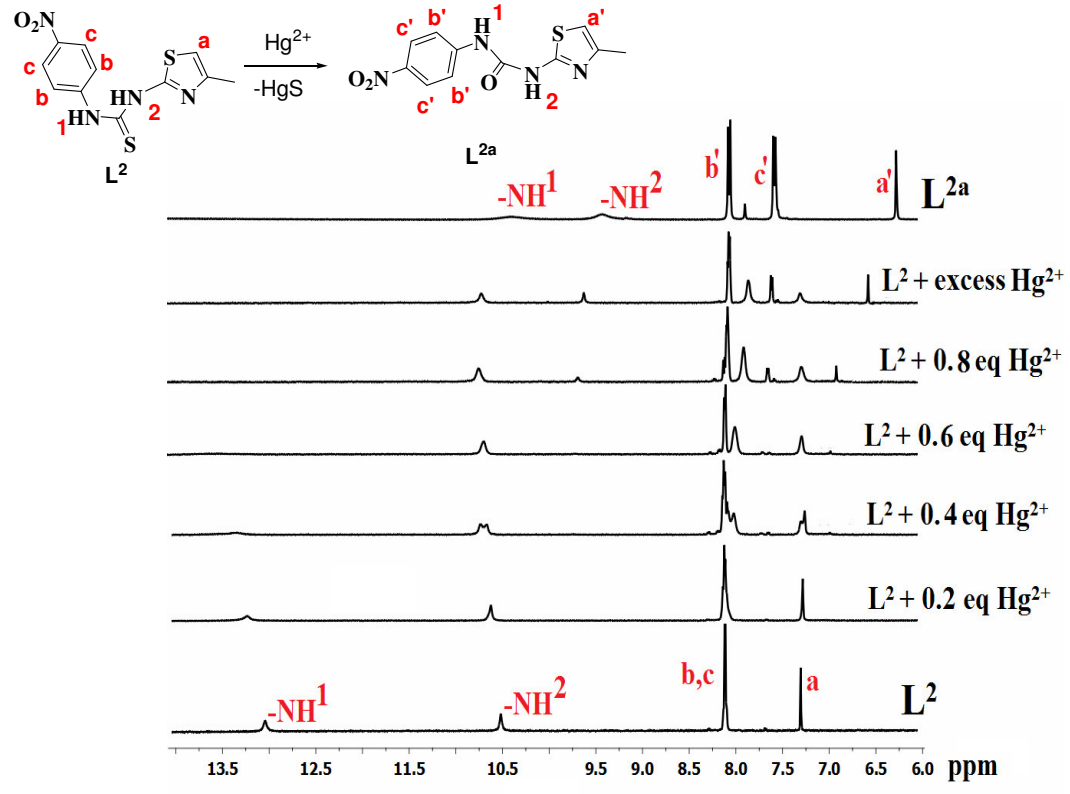

Figure S19: ^{1}H-NMR (DMSO-d^6, 600MHz) spectra (6-14 ppm region) of $\mathbf{L^2}$ during titration with Hg^{2+}.

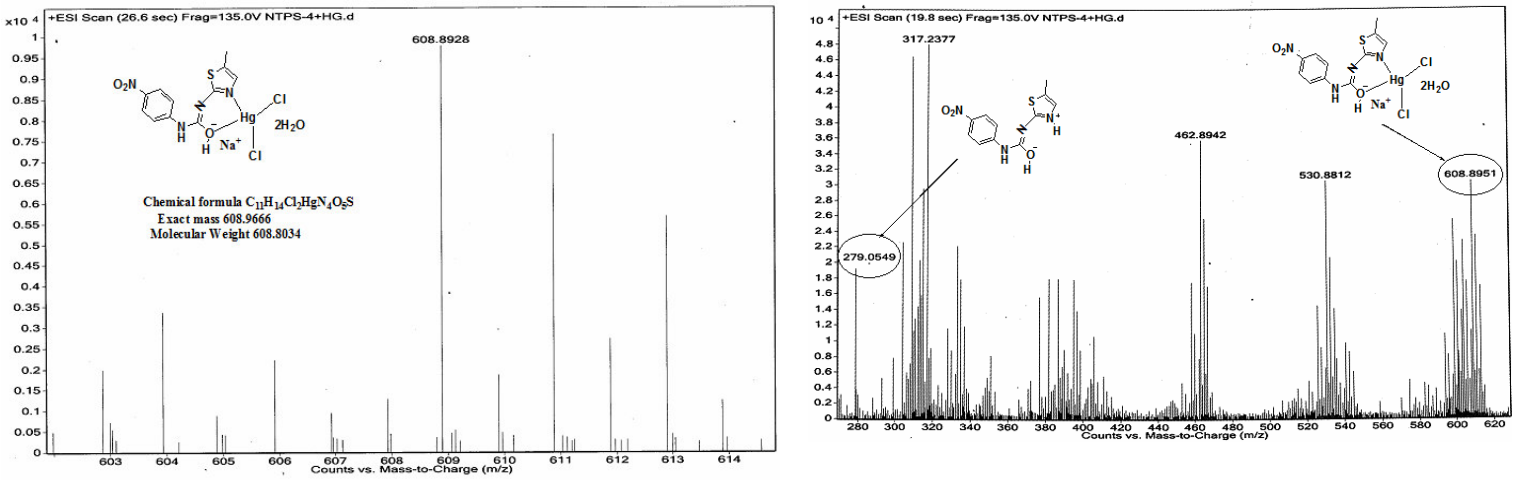

(a) (b)

Figure S20: (a) and (b) are ESI-mass spectra showing two different mass regions of the 1:1 of **L**[1] with mercuric chloride.

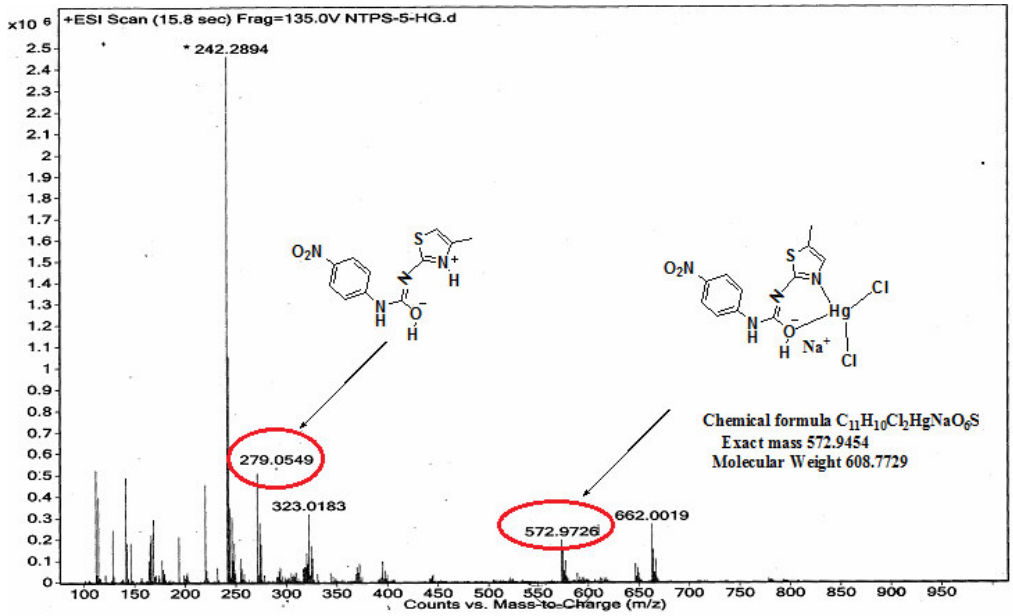

Figure S21**.** ESI-mass spectra of the urea derivative of **L**[2] with $HgCl_2$ showing 1:1 complex formation of urea derivative of **L**[2] with Hg^{2+}.

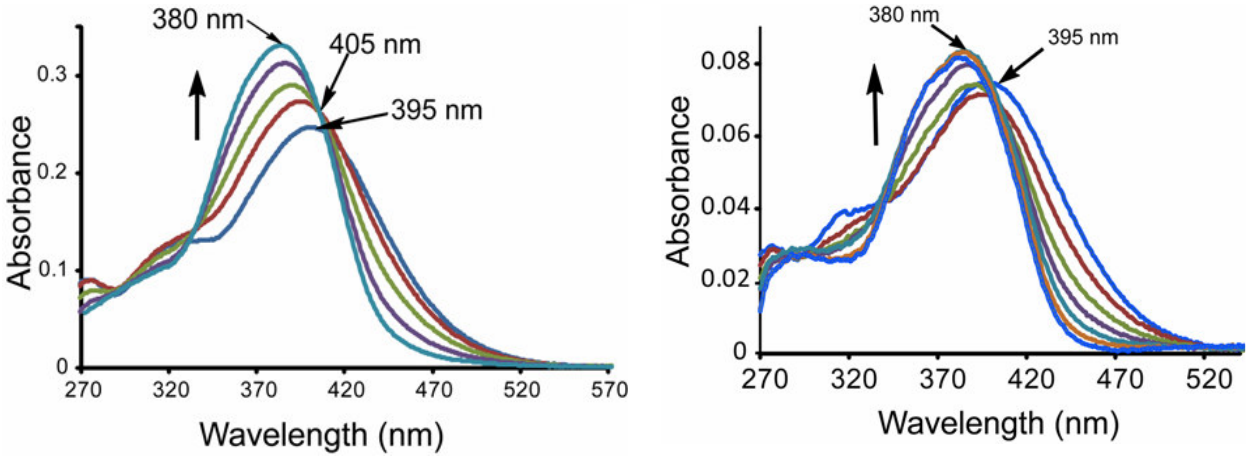

Figure S22: Absorption spectra of (a) $\mathbf{L^1}$ (3 µM) (b) $\mathbf{L^2}$ (1 µM) with Al^{3+} (1 x 10^{-3} M) in dimethylformamide by adding 5µl in each aliquot.

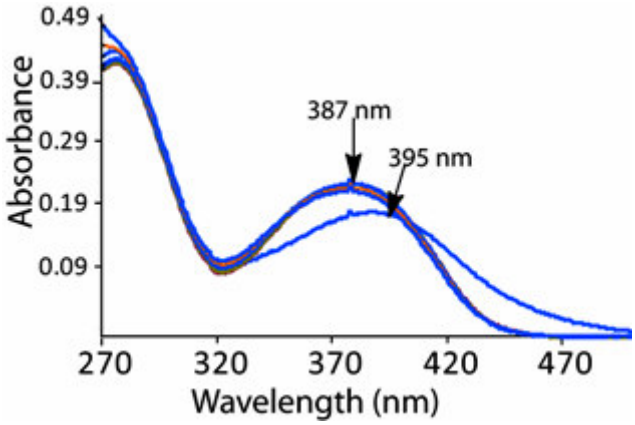

Figure S23: Absorption spectra of (a) $\mathbf{L^1}$ (1 µM) with the addition of Zn^{2+} (1×10^{-2} M) followed by Hg^{2+} (1×10^{-2} M)

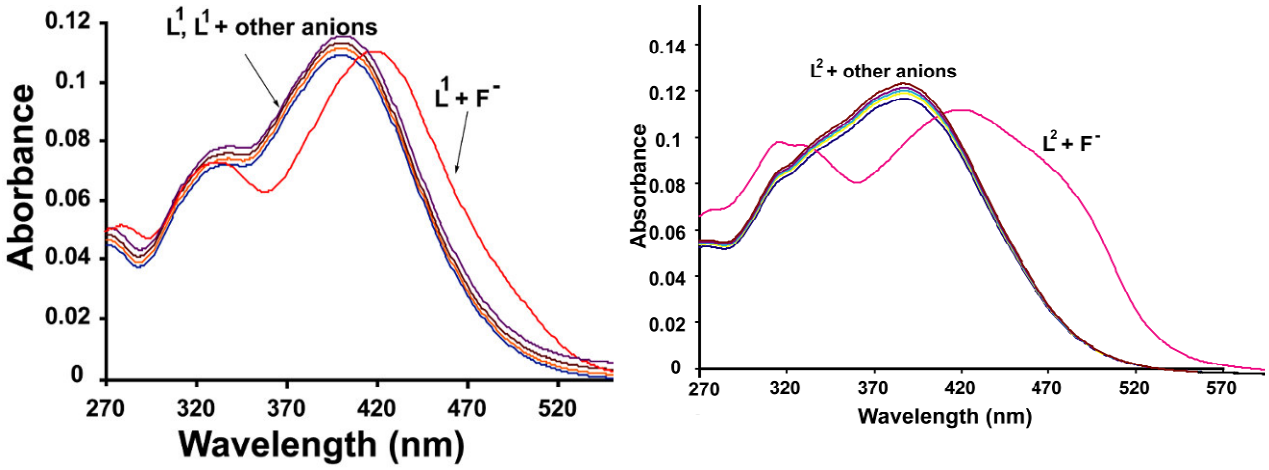

(a) (b)

Figure S24 : UV-visible absorption spectra of (c) $\mathbf{L^1}$ (5 μM) (d) $\mathbf{L^2}$ (7.5 μM) in the presence of different anions such as F^-, Br^-, Cl^-, I^-, SO_4^{2-}, HSO_4^-, PF_6^-, NO_3^-, HPO_4^-, $H_2PO_4^-$, OAc^-, ClO_4^- in DMF (Some lines overlap).

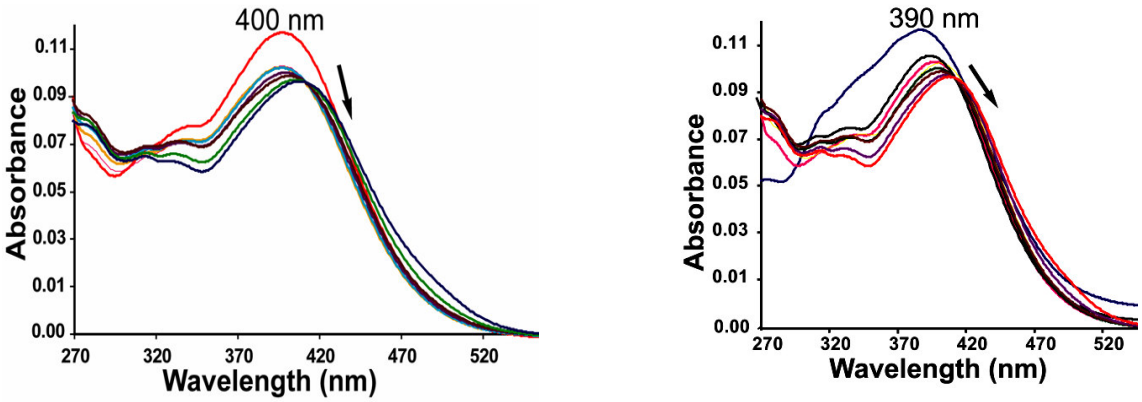

(a) (b)

Figure S25: Absorption spectra of (a) $\mathbf{L^1}$ (1 μM) (b) $\mathbf{L^2}$ (1 μM) with TBAOH in DMF.

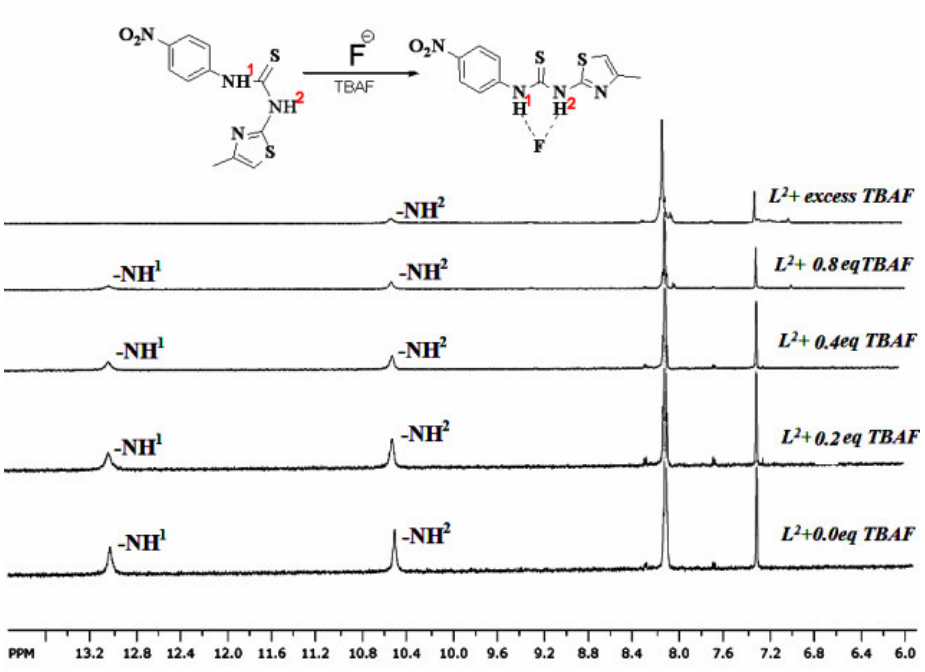

Figure S26: ^{1}H-NMR (DMSO-d^{6}, 600MHz) spectra of aromatic region (6-14ppm) of **L^{2}** during titration with tetrabutylammonium fluoride (0.2, 0.4, 0.6 and 0.8 eq and excess TBAF)

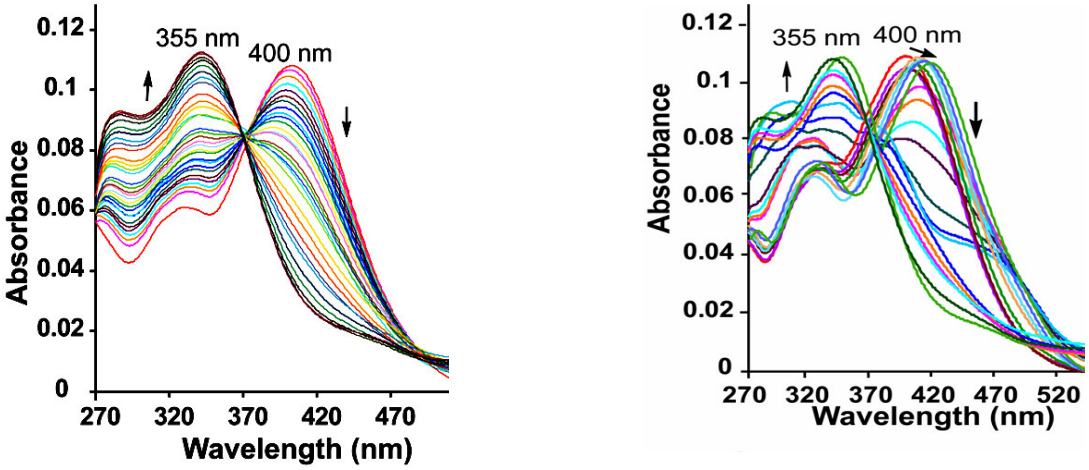

(a) (b)

Figure S27 : Absorption spectra of (a) **L^{1}** (1 μM) on addition of Hg^{2+}(1×10^{-4} M) followed by F^{-} (1×10^{-3} M) (as TBAF); (b) **L^{1}** (1 μM) on addition of F^{-} (1×10^{-4} M) (as TBAF) followed by Hg^{2+}(1×10^{-4} M).

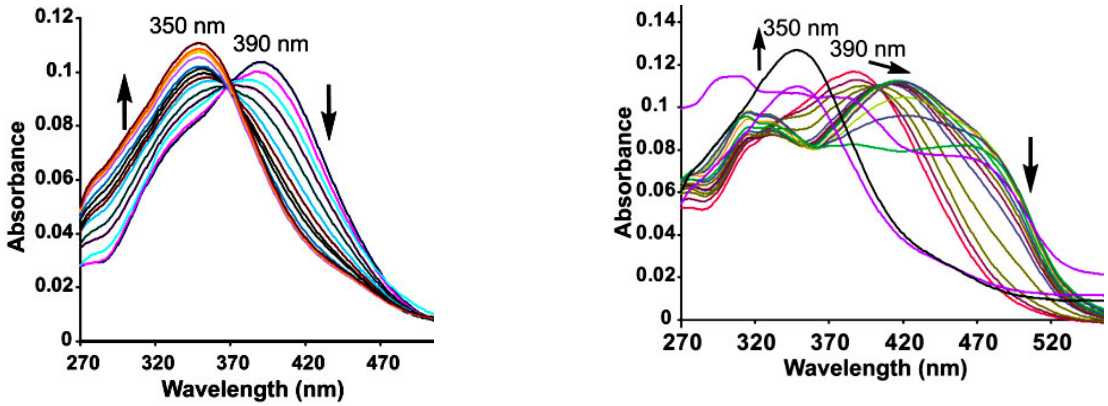

(a) (b)

Figure S28: Absorption spectra of (a) $\mathbf{L^2}$ (1 μM) on addition of Hg^{2+}(1×10^{-3} M) followed by F^- (1×10^{-2} M) (as TBAF); (b) $\mathbf{L^2}$ (1 μM) on addition of F^- (1×10^{-2} M) (as TBAF) followed by Hg^{2+}(1×10^{-3} M).

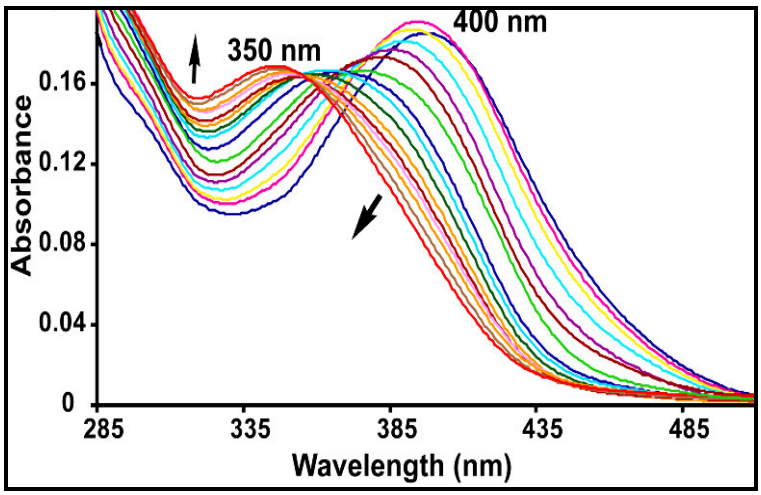

Figure S29 : UV-Visible titration spectra of $\mathbf{L^1}$ (6.0 μM) in at different concentrations of Hg^{2+} (0.31, 0.62, 0.93, 1.2, 1.5, 1.86, 2.16, 2.47, 2.78, 3.08, 3.39, 3.69, 3.99, 4.29, and 4.6μM respectively) at room temperature in DMF/water (9 : 1, v/v) medium

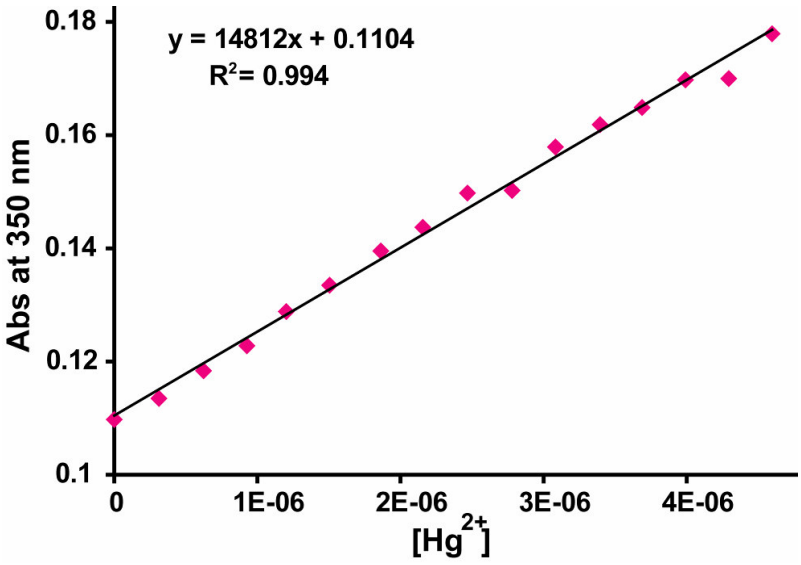

Figure S30: Absorbance versus concentration plot for measuring the detection limit of Hg^{2+} by $\mathbf{L^1}$. (σ = 0.0000753) Detection limit=3.06 ppb

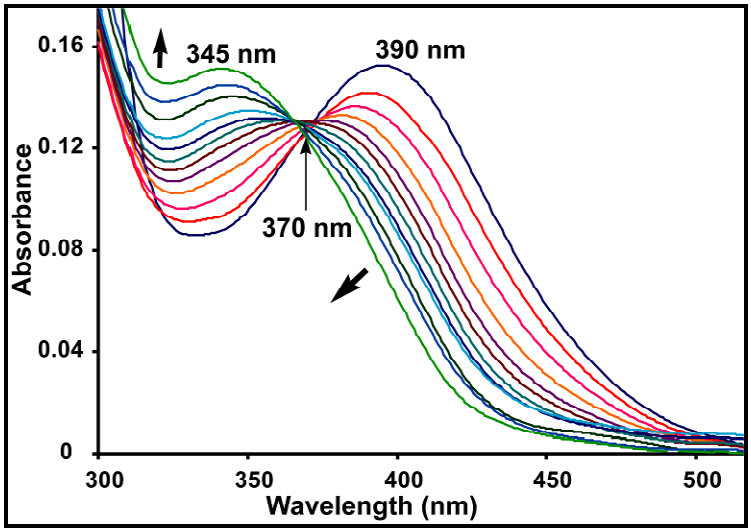

Figure S31 : UV-Visible titration spectra of $\mathbf{L^2}$ (7.5 μM) at different concentrations of Hg^{2+} (0.31, 0.62, 0.93, 1.2, 1.5, 1.86, 2.16, 2.47, 2.78, 3.08 and 3.39 μM respectively) at room temperature in DMF/water (9 : 1, v/v).

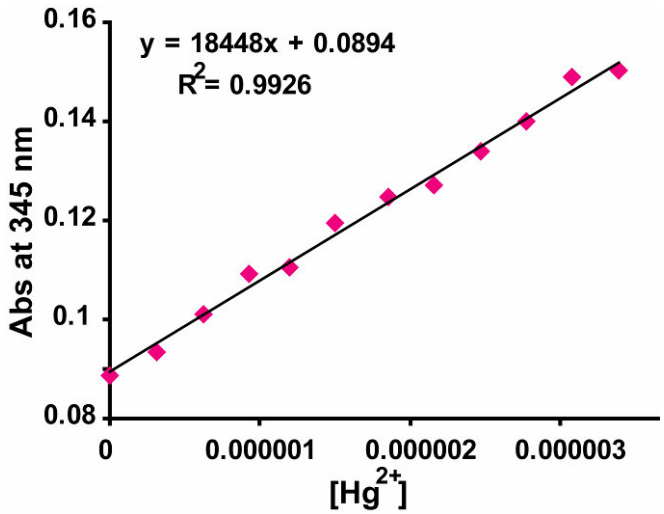

Figure S32: Absorbance versus concentration plot for measuring the detection limit of Hg^{2+} by $\mathbf{L^2}$. (σ = 0.00012111) Detection limit = 4.99 ppb

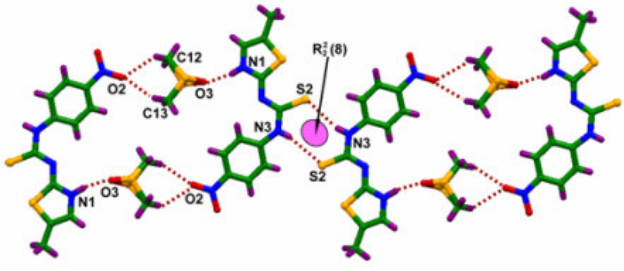

(a)

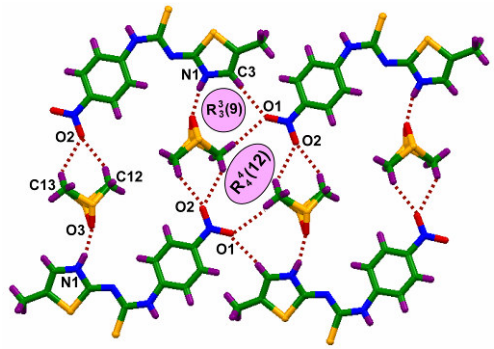

(b)

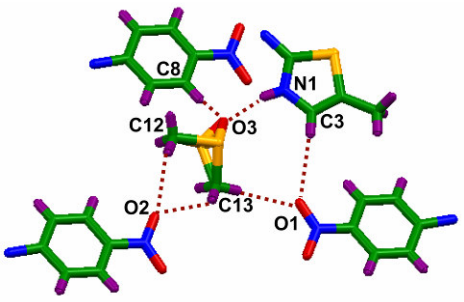

(c)

Figure S33: (a) Various H-bonded assemblies in the crystal lattice of **1a**. (b) Zig-zag arrangement of DMSO molecules in the layers of host molecules. (c) Surroundings of a DMA in **1a**.

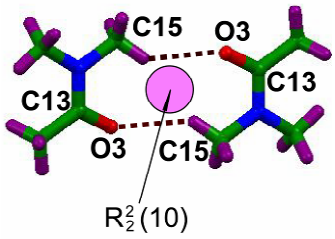

Figure S34: Self-assembly between DMA molecules in the crystal lattice of **2a.**

Figure S35 : Color change of $\mathbf{L^1}$ after addition of F^- and other anions.

Table S1: Crystallographic parameters of $\mathbf{L^1}$, $\mathbf{L^2}$, **1a**, **2a**, **2.1a**, **3a**, **4**, **1b** and **2b**.

Compound No.	$\mathbf{L^1}$	$\mathbf{L^2}$	**1a**	**2a**
Formulae	$C_{11}H_{10}N_4O_2S_2$	$C_{11}H_{10}N_4O_2S_2$	$C_{13}H_{16}N_4O_3S_3$	$C_{15}H_{19}N_5O_3S_2$
Mol. wt.	294.35	294.35	372.48	381.47
Crystal system	Triclinic	Monoclinic	Triclinic	Triclinic
Space group	*P-1*	*C 2/c*	*P-1*	*P-1*
Temperature (K)	296(2)	296(2)	296(2)	296(2)
Wavelength (Å)	0.71073	0.71073	0.71073	0.71073
a (Å)	10.6976(8)	24.0180(18)	7.8556(4)	8.5882(6)
b (Å)	12.5934(9)	4.9616(2)	10.5492(5)	9.0566(7)
c (Å)	14.4096(9)	23.5481(18)	11.5009(6)	13.2569(9)
α (°)	87.490(5)	90.00	91.605(3)	93.909(4)
β (°)	85.965(5)	112.834(9)	102.511(3)	107.379(4)
γ (°)	83.479(5)	90.00	110.839(2)	107.982(4)
V ($Å^3$)	1922.7(2)	2586.3(3)	863.80(8)	921.26(11)
Z	6	8	2	2
Density/Mgm^{-3}	1.525	1.512	1.432	1.375
Abs. Coeff. /mm^{-1}	0.418	0.415	0.447	0.313
Abs. correction	multi-scan	multi-scan	multi-scan	multi-scan
F(000)	912	1216	388	400
Total reflections	6199	2324	3058	3152
Reflections, $I > 2\sigma(I)$	3099	1834	2624	2348
Max. θ/°	25.00	25.25	97.6	25.00

Ranges (h, k, l)	-8 ≤ h ≤ 11 -14 ≤ k ≤ 14 -17 ≤ l ≤ 16	-28 ≤ h ≤ 27 -5 ≤ k ≤ 5 -28 ≤ l ≤ 17	-9 ≤ h ≤ 9 -12 ≤ k ≤ 12 -13 ≤ l ≤ 13	-10 ≤ h ≤ 10 -9 ≤ k ≤ 10 -15 ≤ l ≤ 15
Complete to 2θ (%)	97.5	99.8	97.6	97.3
Data/ restrain/ parameter	6599/0/525	2324/0/181	3058/0/250	3152/0/234
Goof(F^2)	1.003	0.999	1.037	1.036
R indices [$I > 2\sigma(I)$]	0.0577	0.0415	0.0339	0.0398
R indices (all data)	0.1077	0.0572	0.0393	0.0590

Compound No.	**2.1a**	**3a**	**4**	**1b**
Formulae	$C_{15}H_{19}N_5O_3S_2$	$C_{20}H_{26}N_6O_3S$	$C_{27.60}H_{31.60}N_{10}O_6S_4Zn$	$C_{13}H_{15}BrN_4O_4S_2$
Mol. wt.	381.47	430.53	793.06	435.31
Crystal system	Triclinic	Monoclinic	Monoclinic	Triclinic
Space group	*P-1*	*P 2$_1$/n*	*C2/c*	*P-1*
Temperature (K)	296(2)	296(2)	296(2)	296(2)
Wavelength (Å)	0.71073	0.71073	0.71073	0.71073
a (Å)	8.6923(2)	12.7147(16)	35.437(2)	9.2653(7)
b (Å)	9.6622(2)	6.2855(9)	5.1812(3)	10.2683(7)
c (Å)	11.9422(3)	27.243(3)	19.7021(10)	11.4407(8)
α (°)	106.3890(10)	90.00	90.00	66.570(4)
β (°)	91.6680(10)	100.679(9)	94.827(5)	80.387(5)
γ (°)	107.4030(10)	90.00	90.00	65.245(5)
V (Å^3)	911.10(4)	2139.5(5	3604.7(4)	906.93(11)
Z	2	4	4	2
Density/Mgm^{-3}	1.390	1.337	1.461	1.594
Abs. Coeff. /mm^{-1}	0.317	0.186	0.967	2.521
Abs. Correction	multi-scan	multi-scan	multi-scan	multi-scan
F(000)	400	912	1636.8	440
Total reflections	3258	3862	3271	3255
Reflections, $I > 2\sigma(I)$	2775	1513	2266	1699
Max. θ/°	98.5	25.25	25.25	25.25
Ranges (h, k, l)	-10 \≤ h ≤ 10 -11 ≤ k ≤ 11 -14 ≤ l ≤ 14	-15 ≤ h ≤ 14 -7 ≤ k ≤ 7 -32 ≤ l ≤ 32	-42 ≤ h ≤ 42 -6 ≤ k ≤ 4 -23 ≤ l ≤ 12	-11 ≤ h ≤ 11 -12 ≤ k ≤ 11 -13 ≤ l ≤ 13
Complete to 2θ (%)	98.5	99.4	99.8	99.1
Data/ restrain/ parameter	3258/0/289	3862/0/280	3271/0/225	3255 /6/208
Goof(F^2)	1.005	0.817	1.034	1.004
R indices [$I > 2\sigma(I)$]	0.0384	0.0509	0.0571	0.0516
R indices (all data)	0.0444	0.1320	0.0844	0.1286

Compound No.	**2b**
Formulae	$C_{11}H_{12}N_4O_4S$
Mol. wt.	296.31
Crystal system	triclinic
Space group	*P-1*
Temperature (K)	296(2)
Wavelength (Å)	0.71073
a (Å)	6.557(2)
b (Å)	8.595(2)
c (Å)	12.225(3)
α (°)	92.35(2)
β (°)	91.90(2)
γ (°)	98.16(2)
V (Å^3)	680.9(3)
Z	2
Density/Mgm^{-3}	1.445
Abs. Coeff. /mm^{-1}	0.257
Abs. Correction	multi-scan

F(000)	308
Total reflections	2399
Reflections, $I > 2\sigma(I)$	1122
Max. θ/°	25.25
Ranges (h, k, l)	-15 ≤ h ≤ 17 -8 ≤ k ≤ 8 -24 ≤ l ≤ 38
Complete to 2θ (%)	97.3
Data/ restrain/ parameter	2399 /8/190
Goof(F^2)	1.097
R indices [$I > 2\sigma(I)$]	0.1164
R indices (all data)	0.2901

Table S2: Hydrogen bonds parameters of **L^1**, **L^2**, **1a**, **2a**, **2.1.a**, **3a**, **4**, **1b** and **2b**.

Compd No.		$d_{D-H(Å)}$	$d_{H\cdots A(Å)}$	$d_{D\cdots A(Å)}$	∠D-H···A (°)
L^1	N(1)-H(1) ···O(4)	0.86	2.05	2.880(4)	163
	N(3)-H(4A) ···S(4) [x,y,1+z]	0.86	2.74	3.567(4)	161
	N(5)-H(5A) ···O(1)	0.95(4)	1.94(4)	2.876(5)	168(4)
	N(7)-H(7A) ···S(2) [x,y,-1+z]	0.86	2.75	3.596(4)	167
	N(9)-H(9A) ···O(6) [-x,1-y,1-z]	0.82(4)	2.09(4)	2.898(5)	169(4)
	N(11) -H(11A) ···S(6) [-x,1-y,-z]	0.86	2.74	3.576(4)	166
	C(7)-H(7) ···S(4) [x,y,1+z]	0.93	2.84	3.646(4)	146
	C(11)-H(11) ···N(2)	0.93	2.27	2.849(6)	120
	C(18)-H(18) ···N(6)	0.93	2.37	2.892(5)	115
	C(29)-H(29) ···N(10)	0.93	2.32	2.861(5)	117
L2	N(1)-H(1) ···O(1) [-x,1-y,-z]	0.72(3)	2.23(3)	2.946(3)	175(3)
	N(3)-H(3A) ···S(2) [1/2-x,-1/2-y,-z]	0.80(3)	2.76(3)	3.496(3)	154(3)
	C(11)-H(11) ···N(2)	0.93	2.34	2.874(4)	116
1a	N(1)-H(1) ···O(3)	0.86(2)	1.87(2)	2.711(3)	165(2)
	N(3)-H(3A) ···S(2) [-x,-y,1-z]	0.79(2)	2.76(2)	3.5255(19)	163.7(19)
	C(8)-H(8) ···O(3) [1-x,1-y,1-z]	0.93	2.50	3.211(4)	133
	C(11)-H(11) ···N(2)	0.93	2.34	2.901(2)	118
	C(12)-H(12A) ···O(2) [1-x,2-y,1-z]	1.04(4)	2.54(4)	3.318(4)	131(3)
	C(13)-H(13A) ···O(1) [-1+x,y,-1+z]	0.98(4)	2.58(4)	3.564(4)	176(4)
	C(13)-H(13B) ···O(2) [1-x,2-y,1-z]	0.97(4)	2.58(4)	3.280(3)	130(3)
2a	N(1)-H(1) ···O(3)	0.91(3)	1.87(3)	2.764(3)	171(3)
	N(3)-H(3A) ···S(2)	0.86	2.67	3.4918(19)	159
	C(3)-H(3) ···O(2)	0.93	2.57	3.275(4)	133
	C(7)-H(7) ···S(2)	0.93	2.81	3.660(3)	152
	C(11)-H(11) ···N(2)	0.93	2.28	2.851(3)	119
	C(13)-H(13A) ···O(3)	0.96	2.34	2.695(3)	101
2.1a	N(3) -H(1) ···S(2) [1-x,-y,1-z]	0.769(19)	2.820(19)	3.5541(17)	160.5(17)
	N(1)-H(2) ···O(3)	0.88(2)	1.86(2)	2.739(3)	175.6(19)
	C(7)-H(7) ···S(2)	0.93	2.83	3.659(2)	149
	C(8)-H(8) ···O(2)	0.93	2.56	3.305(3)	137
	C(11)-H(11) ···N(2)	0.93	2.32	2.893(2)	120
	C(14)-H(14A)···O(3)	0.87(4)	2.30(3)	2.586(4)	100(3)
3a	N(3)-H(3A) ···O(1)	0.94(3)	2.14(3)	2.982(4)	150(3)
	N(5)-H(5) ···N(1)	0.95(3)	1.91(3)	2.655(4)	134(2)
	C(8)-H(8) ···O(3)	0.93	2.51	3.365(4)	152 121

	C(11)- H(11) ···N(2)	0.93	2.28	2.873(4)	123
	C(12)- H(12A) ···O(1)	0.97	2.47	3.100(3)	
4	N(3) -H(3A) ···O(2A)	0.86	2.09	2.931(7)	165
	C(7) -H(7) ···O(2A)	0.93	2.59	3.358(8)	140
	C(11) -H(11) ···N(2)	0.93	2.25	2.847(6)	121
	C(12) -H(12A) ···O(2A)	0.96	2.46	2.794(11)	100
1b	N(2) -H(2) ···O(4) [-1+x,y,z]	0.86	2.23	3.010(3)	150
	N(3) -H(3) ···O(4) [-1+x,y,z]	0.86	1.96	2.800(3)	165
	C(1) -H(1C) ···Br(1)	0.96	2.89	3.390(3)	114
	C(7) -H(7) ···O(1)	0.93	2.24	2.850(2)	123
	C(12) -H(12B)···N(1) [-x,1-y,-z]	0.96	2.59	3.470(4)	152
	C(13) -H(13C) ···O(1) [1-x,1-y,-z]	0.96	2.51	3.300(3)	139